Thermostructural Analysis of an Experimental Re-entry Vehicle

J. Fatemi

Dutch Space B.V., Newtonweg 1, 2333 CP Leiden, The Netherlands

Abstract: Finite Element (FE) analysis of the Thermal Protection System (TPS) of the European eXPerimental Re-entry Testbed (EXPERT) is presented in this work. The atmospheric re-entry vehicle is subjected to thermal and mechanical loads during its different flight phases, i.e., accelerations, random vibrations, acoustic and shock loads during launch phase, aerodynamic heating and aerodynamic forces during the re-entry phase, and impact shock at the ground impact. Thermal and structural FE models are created to predict the thermal and thermo-mechanical performances of the EXPERT TPS. Geometrical and material non-linearities are accounted for in the FE analyses. The FE analyses results are used for the EXPERT TPS design verification and improvement.

Keywords: Thermal Protection System, Re-entry Vehicle, Thermo-Mechanical Analysis, Thermal stress.

1. Introduction

Atmospheric re-entry vehicles are subjected to severe thermal and mechanical loads during their flight. Considerable accelerations, vibrations, acoustic and shock loads in the launch phase, and aerodynamic heating and aerodynamic forces in the re-entry phase are typical loads which a re-entry vehicle encounters during its mission. To withstand such loads, the vehicle requires a Thermal Protection System (TPS), which is also expected to provide an acceptable aerodynamic surface to avoid early tripping of the high temperature boundary layer (from laminar to turbulent flow). This would significantly increase the thermal heat loads to the structure. An accurate estimation of the temperature distribution over the vehicle TPS during re-entry by means of transient heat transfer analysis is required for a balanced design, meeting both the design and material constraints. The calculated temperatures in combination with aerodynamic forces are used to predict the deformations and thermal and mechanical stresses in the TPS by means of thermo-mechanical analysis. Detailed three-dimensional (3D) thermal and structural Finite Element (FE) models are needed to be developed for the verification of thermal, structural and thermo-mechanical performances of the TPS. The current paper investigates the thermal, structural, and thermo-mechanical FE analyses of the EXPERT TPS.

2. EXPERT vehicle

EXPERT is a re-entry module with the objective of acquiring high-quality hypersonic flight data in relation to critical aero-thermodynamic phenomena that occur during the atmospheric re-entry. EXPERT will be launched by the Russian VOLNA rocket. The major flight events contained in the mission profile of EXPERT are depicted in Figure 1. They are summarized in the following:

- The EXPERT re-entry capsule is launched from a submarine by the VOLNA launcher.
- During the ascent phase, EXPERT is initialized and oriented by the VOLNA 3rd stage and then separated.
- Upon separation from the VOLNA 3rd stage, EXPERT becomes an autonomous system being able to perform a (uncontrolled) ballistic flight with an atmospheric re-entry phase assisted by a parachute system for landing.
- The scientific payloads execute their experiments; EXPERT being in charge of acquiring, recording and transmitting housekeeping and payloads data to Ground.
- Once the scientific phase is completed, EXPERT dumps the scientific data to Ground and executes the procedure to safely land in Kamchatka peninsula landing site.

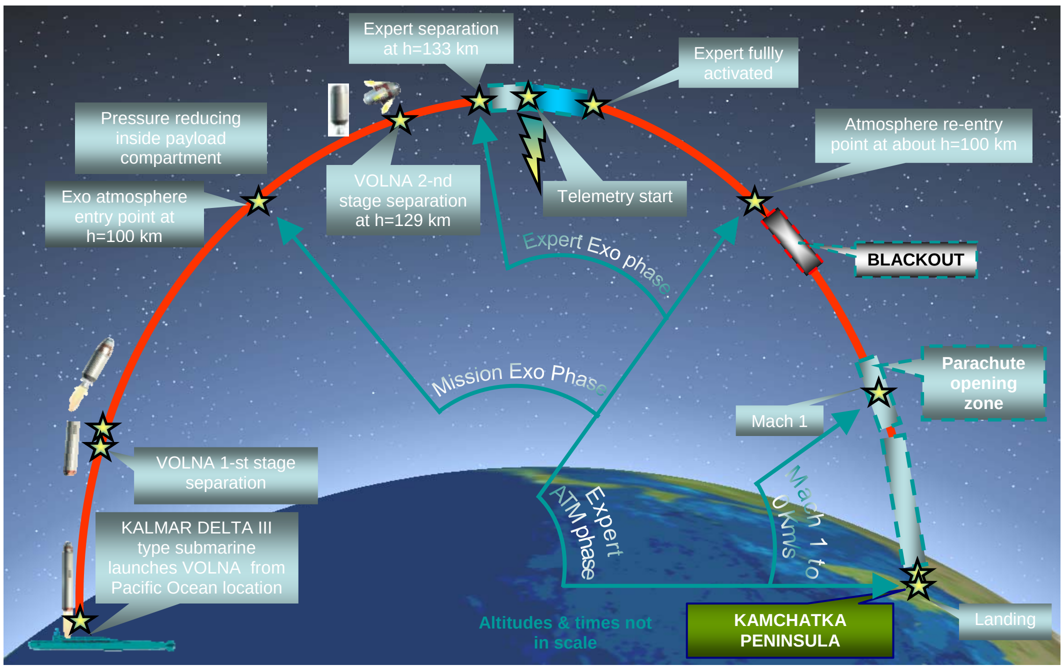

Figure 1. EXPER re-entry vehicle mission profile.

The vehicle TPS is composed of two parts: a CMC nose cap and a metallic conic after-body. The latter is made of the Oxide Dispersion Strengthened (ODS) alloy PM1000, which is a metallic heat resistant material. These materials are selected for high-temperature stability and weight efficiency, while protecting the vehicle structure from the severe entry environment. The metallic TPS is attached to the base-panel (at the vehicle's tail), on which the cold structure is mounted, and to the CMC TPS near the vehicle's nose. The interface between the metallic TPS and nose cap and metallic TPS with base-panel allows thermal expansion of the metallic TPS without introducing excessive thermal stresses in the TPS or interfaces. In order to keep the maximum temperature of the cold structure within the allowable, high temperature insulations are attached to the inner side of the metallic TSP. An overall view of the EXPERT TPS is depicted in Figure 2. The vehicle is 1550 mm high and has a diameter of approximately 1200 mm at its footprint. The cone angle of the vehicle is 25 degrees. The metallic TPS is divided into four curved panels and four flat panels. Four recesses at the bottom of the flat areas are to install the open CMC flaps.

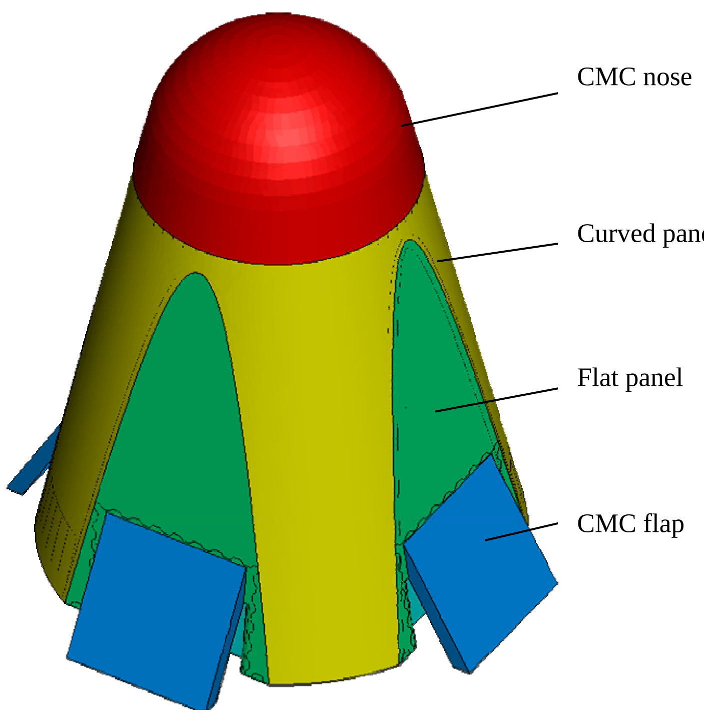

Figure 2. Overall view of EXPERT TPS.

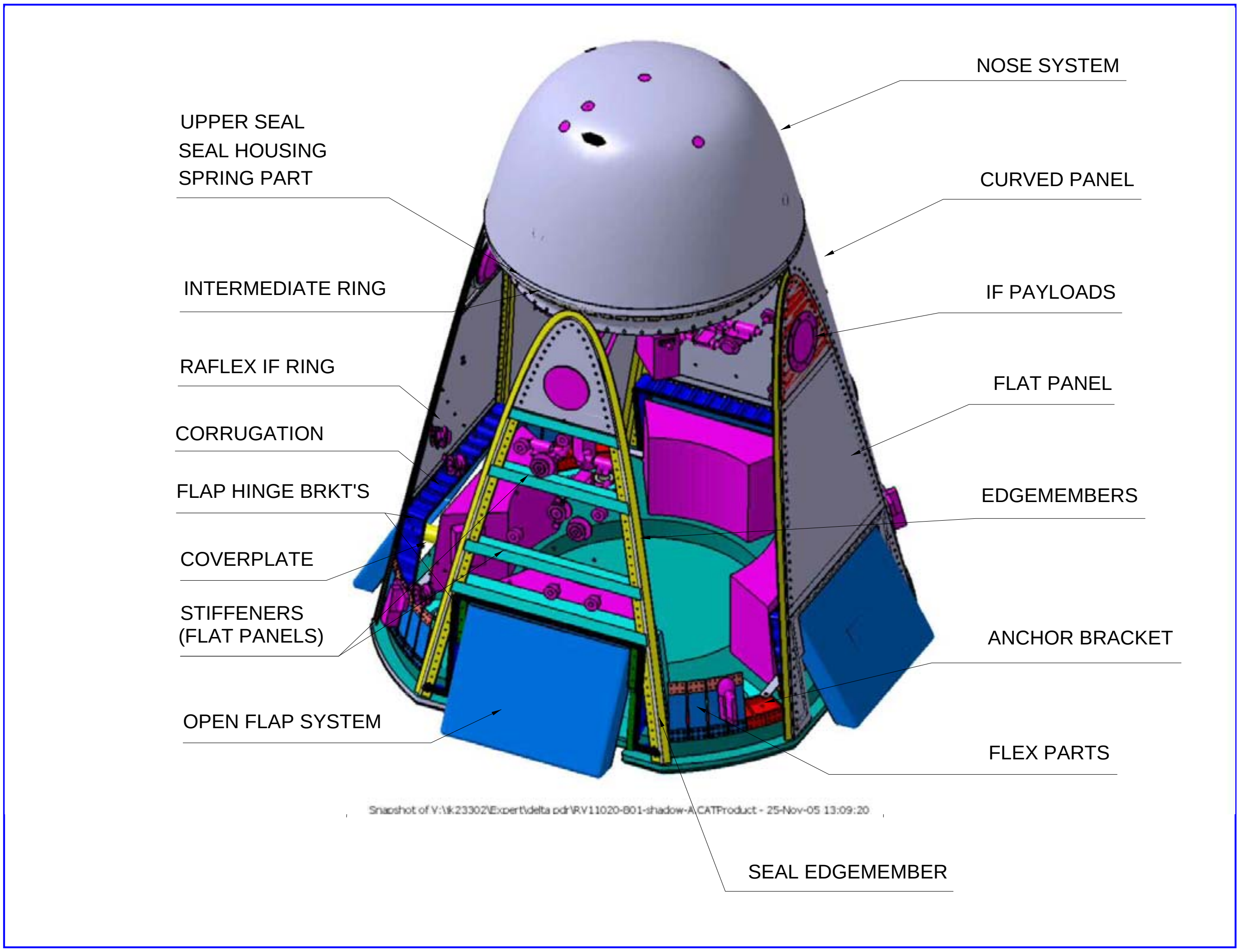

Figure 3. EXPERT TPS design breakdown.

A schematic breakdown of the current design layout with nomenclatures are shown in Figure 3. The structural parts of the TPS are the following:

- Nose sub-system (CMC nose-cap, Colander, Tie-rods, Insulation)
- Intermediate cone and ring
- Outer shell (four curved panels, four flat panels, edge members, four box structures for CMC flaps, four anchor brackets
- Internal insulation
- Seals

3. Material properties

The metallic part of the EXPERT TPS is made of the ODS alloy PM1000. The thermal and mechanical properties of PM1000 are temperature dependent, including isotropic plastic hardening behavior. The mechanical allowables assumed be 3σ corrected values at a given temperature. The hardening law was derived from testing performed at ambient temperature, and scaled proportionally to yield stress for higher temperatures. The nose cap and flaps are made of CMC material. The CMC material is modeled as an elastically isotropic material, having orthotropic expansion coefficients. The thermal expansion coefficient, heat capacity, and thermal conductivity are temperature dependent, although limited availability of data forces linear interpolation between two extreme values.

4. Thermal and Mechanical loads

Technical Specification of the EXPERT TPS specifies the environmental loads to which the TPS sub-system is submitted during its different flight phases. These loads are used as inputs for thermal, structural and thermo-mechanical FE analyses. Three phases can be recognized for derivation of design driving load cases: ground phase, flight phase and re-entry phase. The first phase includes the storage, transportation, integration and handling loads. The second phase incorporates the quasi-static accelerations from the launcher, acoustic loads from the engine, and random vibration and shock loads from the stage separation event. The third phase includes the aerodynamic heating and aerodynamic forces during the atmospheric re-entry and ground impact loads during landing. The mechanical and thermal environment experienced by EXPERT in the ground phase is less severe than the launch and re-entry phases. Therefore, the ground phase loads will not be considered to be dimensioning for the TPS design. The impact analysis of the TPS is not addressed in this work. Two phases are actually dimensioning for the EXPERT TPS design: launch phase and atmospheric re-entry phase. The design driving load-cases to be used as inputs for the thermal and thermo-mechanical FE analyses are defined in the following paragraphs.

4.1 Launch phase

The launch phase of the VOLNA rocket can be split into two sub-phases: the first phase covers the lift-off up to 1^{st}-2^{nd} stage separation, while the second sub-phase covers the stage 2-3 flight up to 2^{nd}-3^{rd} stage separation.

The first launch sub-phase includes the following environments:

- quasi-static accelerations
- sine vibrations
- acoustic pressure loads (including random vibrations)

The second launch sub-phase includes the following environments:

- differential pressure and shock loads (at 2^{nd}-3^{rd} stage separation of launcher)

4.1.1 Launch sub-phase 1

Quasi-static accelerations which also cover the sine vibrations and acoustic pressure which have to be accounted for in the structural FEA of the EXPERT TPS are summarized in Table 1.

Table 1. Quasi-static accelerations.

	Axial	Lateral
Acceleration	+47/-23g	+/-9g

4.1.2 Launch sub-phase 2

During the 2^{nd}-3^{rd} stage separation of the launcher, EXPERT will suddenly undergo a differential pressure of 0.62 bars due to its outer surface exposure to the vacuum. At the same time, EXPERT is subjected to the shock loads during the 2^{nd}-3^{rd} stage separation of VOLNA. Equivalent quasi-static accelerations are calculated to cover the shock loads. These accelerations are summarized in Table 2.

Table 2. Quasi-static accelerations due to 2^{nd}/3^{rd} stage separation of launcher.

	Axial	Lateral
Acceleration	+34/-16g	+/-7g

These two loads (differential pressure, and axial and lateral accelerations) have to be simultaneously applied to the EXPERT TPS for strength and stiffness verifications.

4.2 Atmospheric re-entry phase

The EXPERT TPS is subjected to the aerodynamic heating and aerodynamic forces during the atmospheric re-entry.

4.2.1 Aerodynamic heating loads

The aerodynamic heating loads during the vehicle re-entry are obtained based on a mission for which the re-entry trajectory is characterized by the following parameters:

Entry velocity: 5 km/sec
Entry path angle: -5.5°
Angle of attack: 3.0°
Vehicle mass: 397 kg

The external surface of the TPS is subjected to a transient heat flux during the atmospheric re-entry. The computed heat flux profile, using the Computational Fluid Dynamics (CFD) methods, is applied to the outer surface of the TPS. The heat fluxes presented in this section are defined for specific longitudinal planes of the EXPERT vehicle (Figure 4). These longitudinal reference planes all around the vehicle are considered to derive heat fluxes for TPS design and analysis following a simplified approach that does not consider the 3D distribution. The heat flux distribution for 13 reference planes is plotted in Figure 5 for the time when the stagnation heat flux is maximal. The data which are presented in Figure 5 and Figure 6 are used to interpolate the heat flux profile over the outer surface of the EXPERT TPS in the thermal FE model.

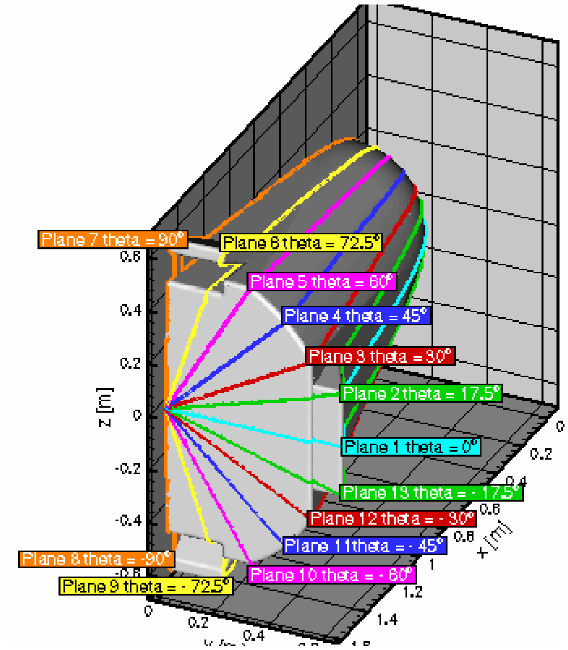

Figure 4. Reference cutting planes for distribution of heat fluxes.

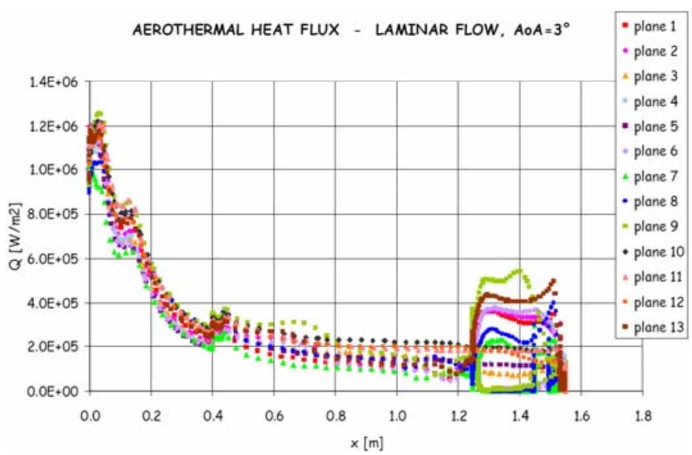

Figure 5. Heat flux distributions for laminar flow.

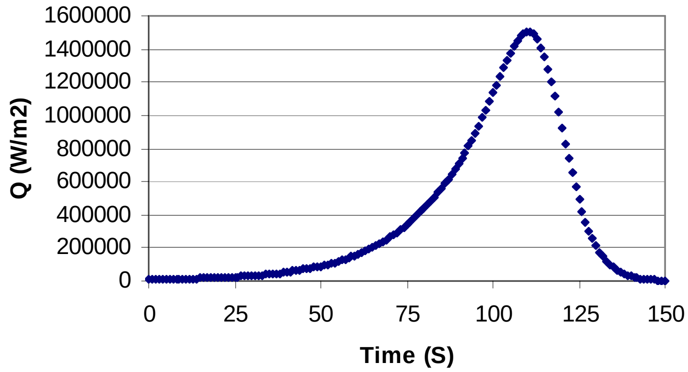

Figure 6. Stagnation heat flux versus time.

4.2.2 Aerodynamic forces

In addition to aerodynamic heating, the outer surface of the EXPERT TPS will be subjected to aerodynamic forces during the atmospheric re-entry. The aerodynamic forces, which incorporate drag and skin friction, decelerate the vehicle. A simplified approach for application of these forces is followed in the actual work. It is assumed that 80% of the total drag and friction forces are applied to the CMC nose. The remaining 20% are not applied to the TPS FE model.

The deceleration force at a given time *t* is calculated by

$$F_{nose} = 0.8 \times m_{total} \times a_x(t) \tag{1}$$

where $m_{total} = 397\ kg$ is the total mass of EXPERT and $a_x(t)$ is a time-dependent deceleration. The maximum deceleration is $a = 16.8g$ at time $t = 121$ second. The time-dependent deceleration force is calculated by multiplying the maximum deceleration (16.8 g) by the normalized dynamic pressure profile. The result of the time-dependent deceleration force which is applied onto the nose cap is shown in Figure 7. The deceleration force profile is applied on the CMC nose.

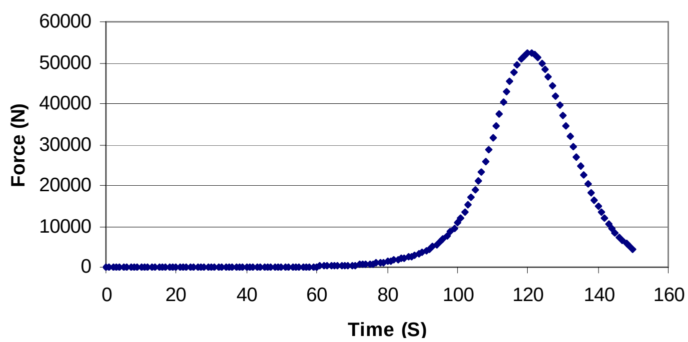

Figure 7. Deceleration force versus time.

5. FE models

This section presents the FE modeling and analysis of the EXPERT TPS. Two separate FE models of the TPS, i.e. thermal FE model and structural FE model, with similar mesh are created. Main assumptions, applied boundary conditions and applied loads of both FE models are discussed in this section. ABAQUS 6.5-4 is used to perform all FE analyses [1].

5.1 Thermal FE model

A 3D heat transfer FE model is developed to calculate the temperature history throughout the TPS structure. Due to radiative heat transfer boundary condition and temperature-dependent thermal properties of materials, the developed FE model is nonlinear. A four-node heat transfer quadrilateral shell element (ABAQUS element DS4), having temperature as degrees-of-freedom, is used to model the TPS structure. Three points through the thickness with linear interpolation are chosen to estimate the temperature gradient through the shell thickness. For the purpose of numerical integration of the FE equations, a 2×2 Gauss integration scheme with a 2×2 nodal integration scheme for the internal energy and specific heat term is used for this element. The thermal FE model has 63636 elements and 71701 nodes. This section is dedicated to explain different aspects of the thermal FE modeling and presents the thermal FEA results.

5.1.1 Initial and boundary conditions

The initial temperature of the entire TPS is assumed to be 273.16 K prior to the atmospheric re-entry. The thermal boundary condition is characterized by the radiation of CMC nose, metallic TPS and CMC flaps to an ambient sink temperature of 273.16 K with an emissivity factor of 0.8. In addition, radiation from flaps to cover boxes, radiation from curved panels to the flexible elements, and radiation from curved and flat panels to the intermediate cone are accounted for. The high temperature insulations are absent in the current FE thermal model. Adiabatic boundary condition is assumed for the internal surfaces of the TPS. The thermal interaction between different parts which are in contact (through rivets and bolts) is taken into account in the thermal FE model. For this purpose, the effective heat transfer conduction between two parts in contact is modeled by means of a “gap conductance parameter”. In this way, the effect of sealing and/or insulations between two parts in contact can be taken into account in the heat transfer analysis. In the actual FE model, the gap conductance is assumed to be very high (i.e. no thermal resistance between parts in contact) due to lack of experimental data. This parameter can later be replaced by the real one once the necessary data from experimental thermal tests are available.

5.1.2 Thermal loads

Transient heat flux as discussed in section 4.2.1 is applied to the outer surface of the TPS. A transient 3D heat flux distribution over the TPS outer surface is determined by developing a dedicated subroutine in ABAQUS. The subroutine first reads the spatial heat flux distributions for different planes of the TPS (Figure 5). Using a linearized interpolation approach, an approximate 3D heat flux distribution over the outer surface of the TPS is then calculated. Finally, the normalized spatial heat flux distribution is multiplied by the time-dependent stagnation point heat flux (Figure 6) in order to determine the transient 3D heat flux distribution over the TPS. During transient FE thermal analysis of EXPERT, the subroutine is called to provide the numerical value of the applied heat flux as a function of time for the corresponding integration point.

5.2 Structural FE model

A 3D structural FE model is developed to predict the mechanical and thermo-mechanical response of the TPS to the applied thermal and mechanical loads during the launch and atmospheric re-entry phases. Geometrical and material nonlinearities are taken into account in the structural FE model. The structural FE model is also used to extract the eigen modes and corresponding mode shapes of the TPS. Four-node linear quadrilateral shell element with reduced integration (ABAQUS element S4R) and enhanced hourglass control is used to model the TPS. The enhanced hourglass control formulation provides improved coarse mesh accuracy with slightly higher computational cost and performs better for nonlinear material response at high strain levels when compared with the default total stiffness formulation. The element has 6 degrees-of-freedom per node (3 translations and 3 rotations), and is robust and suitable for a wide range of applications. The high temperature insulations are taken as non-structural mass in the eigen frequency analysis of the TPS.

5.2.1 Boundary conditions

The structural FE model of the TPS is fully clamped through the lower part of the flexible elements (flex parts in Figure 3). This assumption is justified by the fact that the base-panel is much stiffer than the flexible elements which connect the metallic TPS to the base-panel. The connection of bottom ties (small strips which attach the cover box to anchor bracket) to the anchor brackets (which are absent in the model and assumed to be rigid body) are modeled by hinges. These connectors allow the tie elements to rotate around three axes, but prevent their translations.

5.2.2 Margin of Safety

Margin of Safety (MoS) of different parts of the TPS under different mechanical loads and temperature field are calculated by the following formula:

$$MoS = \frac{allowable\ \ stress}{(applied\ \ stress) \times FoS} - 1 \tag{2}$$

where allowable stress is the temperature-dependent yield stress or ultimate stress, applied stress is the computed von Mises stresses and FoS is the Factor of Safety (1.1 for yield level and 1.25 for ultimate level).

The margins of safety of the TPS structure are calculated for both allowable yield and ultimate stresses for different loadcases. The temperature dependency of yield and ultimate stresses are taken into account in the calculation of MoS. The user-defined subroutine UVARM is developed to calculate the MoS at each integration point through the structural and transient thermo-mechanical FE analyses. In this subroutine, von Mises stress at each integration point is read and compared with the allowable yield and ultimate stresses at the current temperature of each element integration point. At the end of thermo-mechanical analysis, two new output variables (MoS for yield stress and MoS for ultimate stress) are available to be post-processed.

6. FEA results

6.1 Thermal FEA results

Temperature distributions in the TPS during the re-entry phase are presented here. Temperature distributions over the entire TPS and the TPS without nose cap and flaps are shown in Figure 8 and Figure 9, respectively (different legends are used in these pictures). Maximum temperature and corresponding time in nose cap, flaps and metallic TPS are reported in Table 3. As it can be observed, the temperature distribution is not axisymmetric due to an angle of attack of 3° of the vehicle during re-entry. The maximum temperature reaches 1150 K in the windward metallic part near to nose-cone junction.

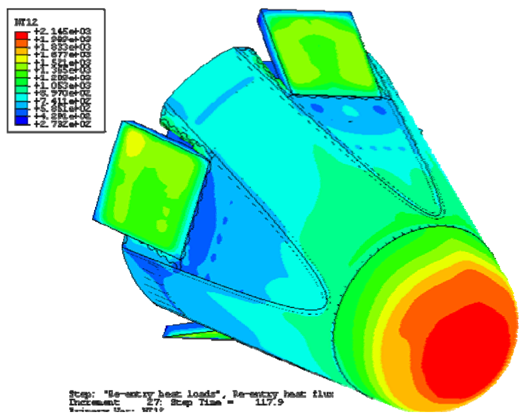

Figure 8. Temperature distributions over the entire TPS.

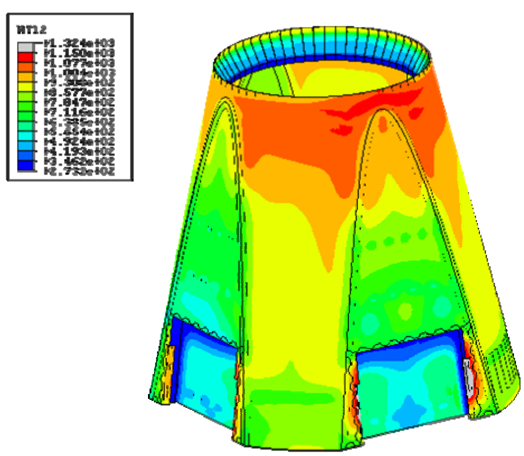

Figure 9. Temperature distribution over the TPS without nose cap and flaps.

Table 3. Maximum temperature and corresponding time for different part of TPS

	Temperature [K]	Time [sec]
CMC nose	2145	118
CMC flap	1595	122
Metallic TPS	1150	125

6.2 Structural FEA results

6.2.1 Eigen frequency

The first 50 eigen frequencies and corresponding mode shapes of the EXPERT TPS are extracted by performing eigen frequency analysis. The extracted lowest eigen frequency of the TPS is 94.5 Hz which is higher than the minimum requirement ($f_{min} = 80$ Hz). This confirms that the TPS design complies with the requirements regarding the lowest frequency. The lowest eigen frequency is related to the vibration of the flap. Figure 10 shows the mode shape of the lowest eigen frequency.

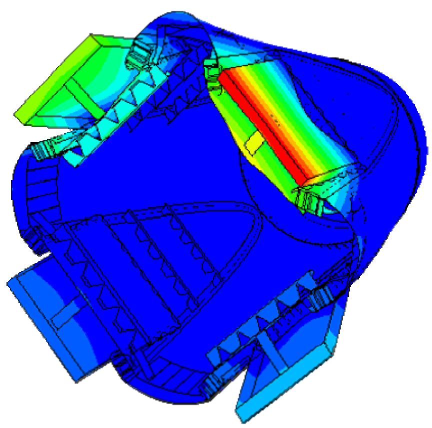

Figure 10. Mode shape of the lowest eigen frequency of TPS ($f = 94.5$ Hz **).**

6.2.2 Structural FEA results

The FEA results of TPS for the current load-case (depressurization in combination with axial and lateral accelerations during the $2^{nd}/3^{rd}$ stage separation of launcher) are presented in this paragraph. Figure 11 shows the displacement distributions (left picture) and von Mises stress distributions (right picture) in the EXPERT TPS. A maximum lateral displacement of 7.1 mm at flap edges is observed. The bottom ties and flat panels near the flap boxes have the highest stresses. The out-ofplane deformation of flat panels is reduced thanks to the flat panels' stiffeners. The positive MoS for the current loads proves that the structure is able to safely withstand such loads.

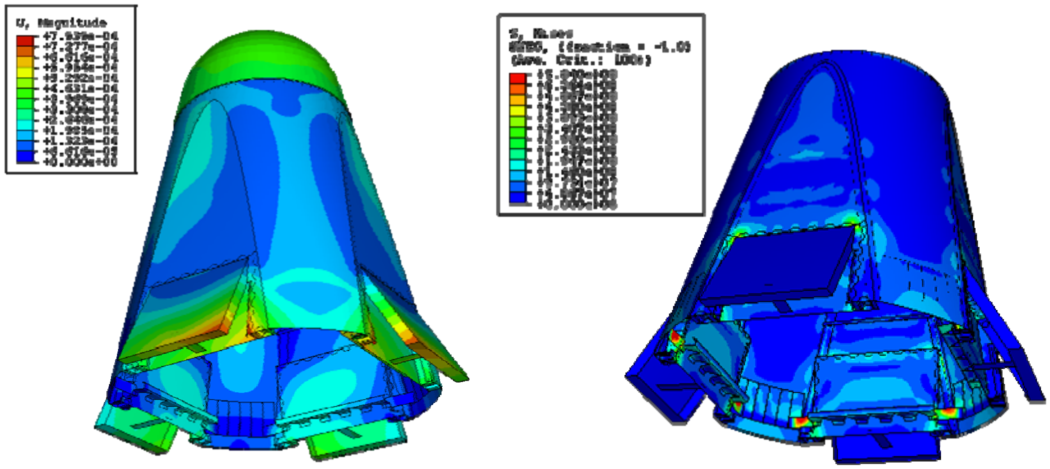

Figure 11. Distribution of displacements (left) and von Mises stresses (right) in TPS.

6.2.3 Thermo-mechanical FEA results

The thermal and mechanical loads during the ammospheric re-entry are the most critical ones for the EXPERT TPS. The vehicle is subjected to severe aerodynamic heating and aerodynamic forces in this phase of the mission. Degradation of mechanical properties of materials with temperature increase will worsen the situation. As it was previously mentioned, providing an acceptable aerodynamic surface to prevent premature transition to turbulent flow is one of the important tasks of a TPS. During the most important phase of the mission (i.e. atmospheric re-entry) the step size and gap size at the junction of CMC nose and metallic TPS change due to different thermal expansions of CMC and PM1000. Figure 12 shows the gap (Δu_a) and step (Δu_r) definitions. Δu_r is the difference in radial thermal expansions between PM1000 TPS and CMC nose (at their junction area) and Δu_a is the difference between the axial displacements of PM1000 TPS and CMC nose at their junction area. The gap size depends on both axial thermal expansion of nose cap and metallic TPS and radial thermal expansion of the metallic TPS. The effects of the former are negligible. The effects of the latter is due to the dedicate design of the mechanical interface (intermediate cone) between nose cap and metallic TPS. The interface is designed such that it provides flexibilities to the metallic TPS for the radial expansion due to thermal loads. As a consequence of radial thermal expansion of the metallic TPS, the interface (intermediate cone) lifts-up the CMC nose to prevent the inter-penetration with the metallic part. The prediction of gap opening during re-entry is of importance for the design of seals between nose and PM1000 TPS. The step size prediction is also important to guarantee that the TPS at the nose-PM1000 TPS junction will not trigger the turbulent flow. As expected, these two parameters vary during the atmospheric re-entry of EXPERT.

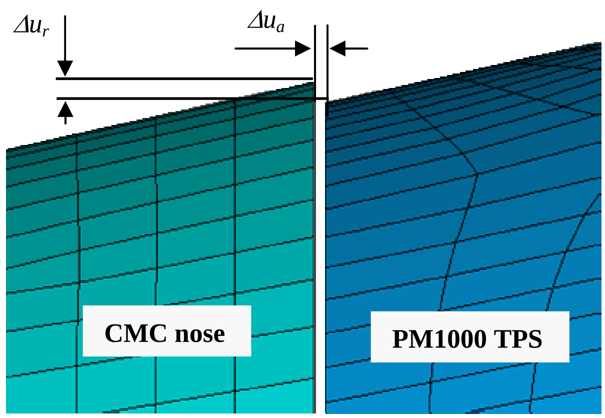

Figure 12. Gap and step definition at the CMC nose and PM1000 TPS junction.

Displacements

Mach number, step size and gap size evolution during the re-entry phase are shown in Figure 13. Maximum step size and gap size reach 4 mm and 1 mm, respectively, at 125 seconds from re-entry. These values can be used to fine-tune the TPS design (initial step size and gap size) such that the design complies with the requirements.

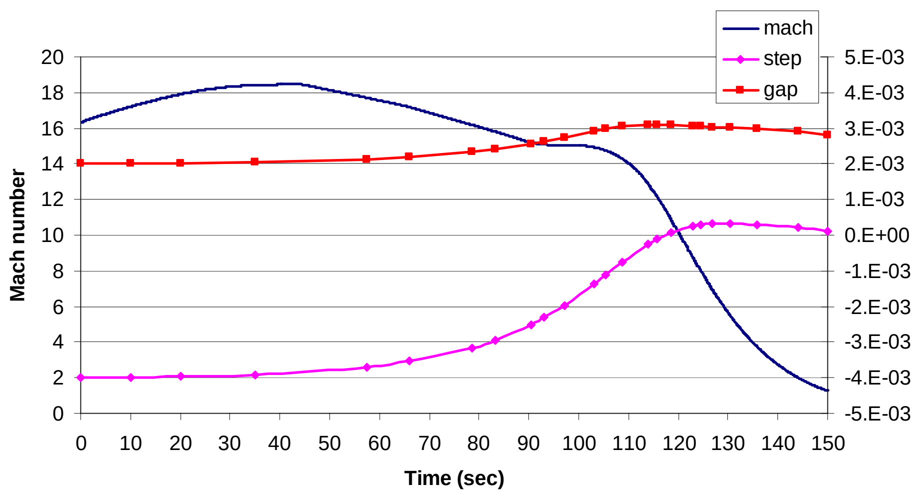

Figure 13. Mach number, step and gap size versus time.

Stresses

The stress distribution in different parts of the TPS due to the applied temperature field in combination with deceleration forces are presented in this paragraph.

a) *Intermediate cone*

Due to the thermal loads, the intermediate cone experiences high temperature gradient which consequently induces thermal stresses. In addition, thermal expansion of the metallic TPS induces bending stresses in the intermediate cone. The compression forces on the nose cap due to deceleration of the vehicle will consequently create tension (in axial direction of EXPERT) in the intermediate cone. This combination of loads creates high stresses in the intermediate cone near the metallic TPS junction. Figure 14 shows the distribution of von Mises stresses in the intermediate cone at 121 second from re-entry, when the deceleration forces are maximal. Maximum equivalent plastic strain of 0.5% is observed in the intermediate cone.

b) *Curved and flat panels and flap box*

Figure 15 shows the von Mises stress distribution in the curved and flat panels and flap boxes assembly. High von Mises stresses are observed in the attachment areas of curved and flat panel through the edge-members. The high stresses in such areas are due to the thermal expansion mismatch between panels and edge-member. The edge-member is continuous in the actual FE model, but discontinuous in the real design. The stresses are expected to be reduced once the FE model is updated. High von Mises stresses are also observed in the flap boxes (see Figure 15) due to a high temperature gradient (see Figure 9 for temperature distributions).

c) *Flexible elements*

The flexible elements are highly loaded in compression as a result of deceleration loads. Radial thermal expansion of the metallic TPS bends these elements. Combination of high compression forces and bent shape creates high stresses in the flexible elements and increases the risk of buckling. Distribution of von Mises stresses in the flexible elements is shown in Figure 16. The stress level and deformed shape of the flexible elements show that these elements are quite robust and can withstand the re-entry loads.

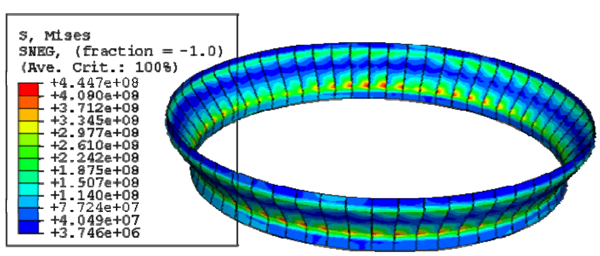

Figure 14. Distribution of von Mises stresses in intermediate cone.

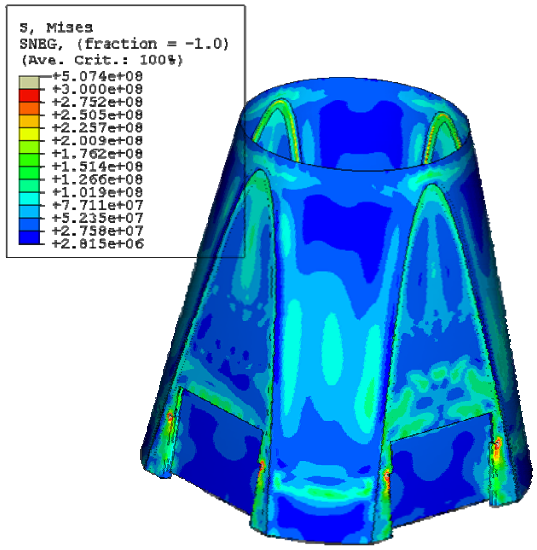

Figure 15. Distribution of von Mises stresses in TPS.

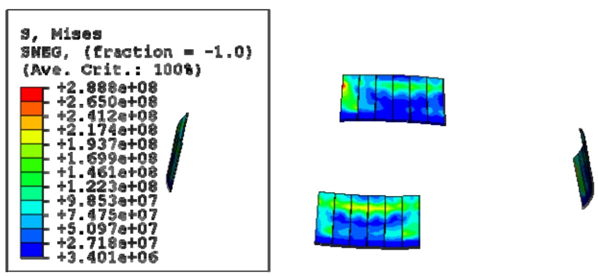

Figure 16. Distribution of von Mises stresses

Margins of safety

Margins of safety (based on both yield and ultimate stresses) for different parts of the TPS are calculated during the transient thermo-mechanical FE analysis. To have a clear idea of the thermo-mechanical performances of the TPS, the margins of safety are represented graphically for the re-entry loads. Figure 17 depicts the MoS (based on yield stress) for the whole metallic TPS. This Figure shows the lowest MoS at each integration point of finite elements for re-entry loads. The *min* and *max* values (lower and upper bounds) of MoS set to 0 and 1 in the legend correspond to red and blue colors, respectively. Colors above 1 and under 0 are presented with grey and black, respectively. Therefore, the regions with grey color represent MoS greater than 1 and with black color negative MoS. As it can be observed, almost the whole TPS has positive MoS except a few local areas. Local modifications of the current TPS design can improve the performance of the TPS in such areas. Refinement of the FE model in such areas can also improve the prediction of the thermal and thermo-mechanical performances of the TPS.

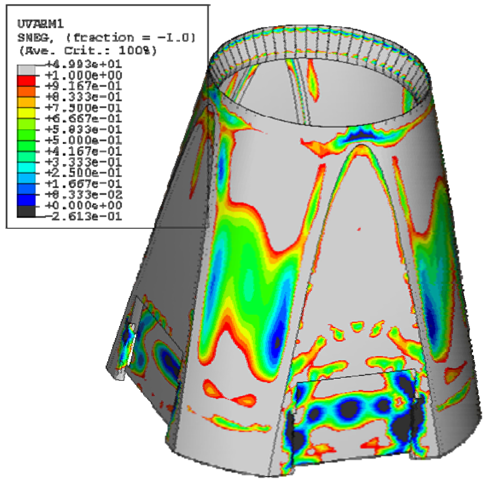

Figure 17. MoS based on yield stress for the metallic TPS subjected to re-entry loads.

7. Concluding remarks

Nonlinear FE analyses were performed to predict the thermal, structural and thermo-mechanical behavior of the EXPERT TPS. Thermal and mechanical loads during the launch phase and re-entry phase were described. Main assumptions and different aspects of the FE modeling of the TPS were addressed, and the results of the thermal, structural and thermo-mechanical FE analyses of the TPS were presented.

The results of the transient heat transfer analysis showed that the maximum temperature in different materials (CMC nose, CMC flaps and PM1000 TPS) remains below the maximum allowable temperatures as mentioned in the design requirements.

The results of the structural analysis showed that the structure can withstand the launch loads (accelerations, depressurization and shock loads). High margins of safety for the TPS were found for the launch loads.

The results of the transient thermo-mechanical analysis showed that the re-entry loads are the most critical ones for the EXPERT TPS. Although the actual TPS concept withstands the combination of thermal and mechanical loads during the re-entry phase, local modifications of the actual design are needed to improve the thermo-mechanical performances of the TPS. Local FE models (more detailed FE models) are also needed to be developed for more accurate prediction of thermal and structural behavior of the TPS.

8. References

1. ABAQUS User’s Manual, Version 6.5, 2005.